Grad-Shafranov Equilibria with Negative Core Toroidal Current in Tokamak Plasmas

Paulo Rodrigues* and João P. S. Bizarro†

Centro de Fusão Nuclear, Associação Euratom—IST, Instituto Superior Técnico, 1049-001 Lisboa, Portugal

(Received 1 February 2005; published 27 June 2005)

Numerical Grad-Shafranov (GS) equilibria with negative current density in the plasma core are computed which do not impose any particularly chosen models for the pressure and current-density profiles. This flexibility allows the profiles to be tailored so that an island unfolds in the low-field side, even for elongated plasmas, thus sustaining the negative-current core against outward forces. Among other topological results, reversed GS equilibria are also shown to be necessarily non-nested, except for the cylindrical and other very special degenerate, hence structurally unstable cases.

DOI: 10.1103/PhysRevLett.95.015001 PACS numbers: 28.52.Av, 52.55.Fa, 52.65.Kj, 52.65.Vv

Driving of large off-axis, noninductive plasma current in tokamak experiments has led to improved confinement regimes, with strongly reversed magnetic shear and nearly zero toroidal current density near the magnetic axis [1,2]. Although current-drive power often suffices to decrease the core current density further into negative values, available data shows the latter to be clamped at zero, possibly due to axisymmetric reconnection events [3,4]. This attracted considerable discussion in the fusion community about possible Grad-Shafranov (GS) reversed equilibria, with negative toroidal current density flowing in the core and overall positive plasma current. Inducing a poloidal-field reversal (PFR) layer, for which the tangential magnetic field and the enclosed toroidal current do vanish, such equilibria were deemed impossible [5]. After suitable revisions, nested reversed equilibria have been claimed to be possible but isolated and structurally unstable, in the sense that any slight change in boundary conditions would cause their destruction [6]. Subsequently, it was recognized that non-nested configurations could sustain a negative-current core [7], this being supported by GS solutions for particularly chosen pressure and current-density models [8,9]. Despite their role in asserting that GS equilibria can exhibit current reversal, these works are rather limited in scope, their reliance on particular models hindering the extrapolation to reactorlike plasmas and obscuring the underlying physics, whence the need to tackle more general profiles. Indeed, existing numerical solutions can only cope with flat pressure and current-density profiles [8], whereas known analytical solutions are restricted to quite stiff models that force negative current densities also in regions other than the plasma core [9].

In this Letter, some relevant features of GS equilibria with toroidal current reversal are discussed. First, nested configurations are shown to be special degenerate cases, their isolated character being the key to understanding why structurally stable, realizable, nonsingular solutions are necessarily non-nested. Next, a perturbative GS equilibrium solver [10], able to deal with realistic pressure and current-density profiles, is adapted to handle the PFR layer, providing insight about the problems due to a vanishing poloidal field inside the plasma. Namely, it is shown that pressure and poloidal-field input profiles cannot be arbitrarily chosen. More, it is found that the usual resilient current-density distributions [11–13] are not allowed, which may account for reconnection events aiming to eliminate the negative current and drive the equilibrium towards a nested, nonreversed configuration. Still, and as previously hinted [14], such events can be countered by a suitably shaped internal separatrix, which is achieved below by tailoring the pressure and poloidal-field input profiles. In the following, standard notation will be used, with superscripts B^i and subscripts B_i denoting, respectively, contravariant and covariant components of a given vector $\mathbf{B} = B_{(i)}\mathbf{e}_i$.

Let $\psi(r, \theta; \varepsilon)$ be a solution of the GS equation

$$-R^2\nabla\cdot(R^{-2}\nabla\psi) \equiv -J_\phi(r,\theta) \equiv R^2\dot{p}(\psi) + \dot{Y}(\psi) \quad (1)$$

for a given value of the inverse aspect ratio $\varepsilon = a/R_0$, with a and R_0 the tokamak minor and major radius, respectively, the dot denoting flux derivatives $d/d\psi$ and the normalized poloidal-field flux ψ, plasma pressure $p(\psi)$, squared poloidal current $Y(\psi)$, and toroidal current density $J_{(\phi)}$, along with the toroidal coordinate system (r, θ, ϕ) and $R = 1 - \varepsilon r\cos\theta$, being defined as in previous work [10]. An equilibrium topology is nested around the origin if a smooth application exists, with nonsingular Jacobian $\sqrt{g}$ (except on $r = 0$), which maps the space into flux coordinates $(\varrho, \vartheta, \phi)$ such that $\psi(r, \theta) = \psi(\varrho)$. The toroidal current enclosed by each flux surface, $I(\varrho) = \int_0^\varrho \times \int_{-\pi}^{\pi}\sqrt{g}J^\phi(\varrho', \vartheta')d\vartheta' d\varrho'$, is then continuous on the flux label ϱ and the PFR layer matches a given flux surface. There, Ampère's Law requires $\oint B_\vartheta d\vartheta = 0$, with $B^i = \epsilon^{i\phi j}\partial_j\psi$ the field poloidal-section components and ϵ^{ijk} the Levi-Civita tensor, whence $d\psi/d\varrho = 0$ because $\oint g_{\vartheta\vartheta}/\sqrt{g}d\vartheta$ is always positive. In addition to symmetry in the angle ϑ, this forces $\nabla\psi$ to vanish and the Hessian matrix $\partial^2_{ij}\psi$, with eigenvalues $\lambda_\varrho = g_{\varrho\varrho}J_\phi$ and $\lambda_\vartheta = 0$, to be singular throughout the PFR layer, thus defining the latter as a set of degenerate critical points. On the other hand, it is known that values of the control parameter ε for

which $\psi(r,\theta;\varepsilon)$ displays degenerate critical points always make up a measure-zero set in parameter space (the bifurcation set) [15]. Moreover, corresponding degenerate functions are structurally unstable, and any small perturbation in ε turns the connected set of degenerate critical points into a discrete set of isolated, nondegenerate ones, in whose vicinity $\psi(r,\theta;\varepsilon)$ is reduced to a twofold Morse form (e.g., an o point or a x point) [16]. Hence, reversed equilibria with nested topology are isolated and hardly realizable, as previously reported [6], while structurally stable non-nested solutions should be expected whenever ε leaves its bifurcation set, which is reduced to $\varepsilon = 0$ if solutions for Eq. (1) are sought as

$$\psi(r,\theta;\varepsilon) = \psi_0(r) + \sum_{n=1}^{+\infty}\sum_{k=0}^{n}\frac{\varepsilon^n}{n!}\hat{\psi}_{nk}(r)\cos k\theta, \qquad (2)$$

and if the very peculiar boundary conditions and input profiles that would arise from setting $\det(\partial^2_{ij}\psi) = 0$ with nonzero ε are excluded. Then, departing from cylindrical equilibria, an island system unfolds from the once degenerate PFR layer, precluding a global mapping to flux coordinates and yielding a jump in $I(\varrho)$ every time a separatrix is crossed. Note that every flux surface must now enclose a nonvanishing toroidal current (otherwise it would be a set of degenerate critical points), and the PFR layer becomes orthogonal to all unfolding flux surfaces.

Inserting the series (2) into Eq. (1), and subsequently collecting for the same powers of ε, is known to engender the zeroth-order condition

$$-\frac{1}{r}\frac{d}{dr}[r\psi_0'(r)] = \dot{p}_0(r) + \dot{Y}_0(r) \qquad (3)$$

and the ordinary-differential-equation hierarchy

$$r^2\hat{\psi}_{nk}''(r) + r\hat{\psi}_{nk}'(r) + [s(r) - k^2]\hat{\psi}_{nk}(r) = \hat{b}_{nk}(r), \qquad (4)$$

where $s(r) = r^2[\ddot{p}_0(r) + \ddot{Y}_0(r)]$ and the nonhomogeneous term $\hat{b}_{nk}(r)$ couples lower-order quantities only, allowing each $\hat{\psi}_{nk}(r)$ to be computed in a closed integral form as

$$\hat{\psi}_{nk}(r) = g_k(r)\left[\frac{\hat{\psi}^*_{nk}}{g^*_k} + \int_{r^*_{nk}}^{r} du\, u^{-1} g_k^{-2}(u) \times \int_0^u dv\, v^{-1} g_k(v)\hat{b}_{nk}(v)\right], \qquad (5)$$

once input profiles [the zeroth-order pressure $p_0(r)$ and poloidal field $\psi_0'(r)$], homogeneous solutions $g_k(r)$ to Eq. (4), and boundary conditions $\hat{\psi}^*_{nk} = \hat{\psi}_{nk}(r^*_{nk})$ at $r^*_{nk} > 0$ are provided (except for $k \le 1$, where $r^*_{nk} = \hat{\psi}^*_{nk} = 0$) [10]. It is also known that $p_0(r) = p[\psi(r,\theta_p)]$ and $\psi_0'(r) = \partial_r\psi(r,\theta_B)$ are not changed along the chords θ_p and θ_B, when considering successive perturbations $\hat{\psi}_{nk}(r)$, if additional dependencies in ε for $p(\psi,\varepsilon)$ and $Y(\psi,\varepsilon)$ are suitably defined, enabling a natural relation with experimental data [10]. Although each $\mathcal{P}_n(r) = \partial^n p(\psi,\varepsilon)/\partial\varepsilon^n|_{\varepsilon=0}$ and $\mathcal{Y}_n(r) = \partial^n Y(\psi,\varepsilon)/\partial\varepsilon^n|_{\varepsilon=0}$ is, by definition, a function of $\psi_0(r)$, they are required to annihilate a set of arbitrary radial functions [10], which is possible only if $\psi_0'(r)$ never vanishes and the inverse function $r(\psi_0)$ does exist. Therefore, reversed equilibria cannot be easily handled and the additional dependencies in ε for $p(\psi)$ and $Y(\psi)$ must be dropped, leaving $p[\psi(r,\theta)]$ and $\partial_r\psi(r,\theta)$ subject everywhere to the effects of all perturbations $\hat{\psi}_{nk}(r)$, including also over any chords θ_p and θ_B.

Following directly from Eqs. (1) and (3), the zeroth-order profile $J_0^\phi(r) = r^{-1}d(r\psi_0')/dr$ must be a function of $\psi_0(r)$ with well defined flux derivatives $(d/d\psi_0)^n J_0^\phi(\psi_0) = (1/\psi_0')(d/dr)(d/d\psi_0)^{n-1}J_0^\phi[\psi_0(r)]$. Such is indeed the case for any radial function $J_0^\phi(r)$ if ψ_0' never vanishes, whereas for a reversed configuration [with $\psi_0'(r_L) = 0$ at $r_L > 0$] care must be taken to ensure that ψ_0' does not approach zero over r_L faster than $(d/dr)(d/d\psi_0)^n J_0^\phi(\psi_0)$ for every $n \ge 0$. To this end, the nonlinear condition

$$r^2\psi_0''(r) + r\psi_0'(r) = r^2 J_0^\phi[\psi_0(r)] \qquad (6)$$

must be solved for some $J_0^\phi(\psi_0)$ with a proper Taylor series expansion at $\psi_L = \psi_0(r_L)$, along with the conditions $\psi_0(0) = \psi_0'(r_L) = 0$, which means the zeroth-order poloidal field $B_0^\theta(r) = r^{-1}\psi_0'(r)$ cannot be arbitrarily chosen. Moreover, every PFR layer point (except the x points) is enclosed by a set of unfolding flux surfaces, which are pierced twice (on both sides of the layer) by any chord $\theta = \theta_f$ directed towards the core. Consequently, the radial profile $f(r) = f[\psi(r,\theta_f)]$ for any continuously differentiable flux function $f(\psi)$ cannot be monotonic, as the derivative $f'(r) = \dot{f}(\psi)\partial_r\psi$ does change its sign when crossing the PFR layer. Applied to $p(\psi)$, this simple argument properly extends previous results [6,7,9] to non-nested equilibria and general input profiles.

Current-carrying plasmas are known to display preferred (or resilient) current-density profiles of the type $J_0^\phi(\psi_0) \propto e^{-\lambda\psi_0}$, and several attempts have been made to derive these from some variational or statistical principle [11–13]. Leading to $\psi_0(r) \propto \ln[1 + (e^{\lambda/2} - 1)r^2]$, such profiles cannot sustain a PFR layer, because neither $J_0^\phi(\psi_0)$ nor $\psi_0'(r)$ would be allowed to reverse their sign. A natural relaxation should then be expected, driving the reversed equilibria towards a resilient distribution while removing the PFR layer. This process is visible in nonlinear resistive simulations [17], with the negative-current region enclosing the magnetic axis being displaced towards the low-field-side x point, where the two critical points merge together and vanish with a sudden change in equilibrium topology. Yet, relaxation events may be halted if the low-field-side x point is turned into an o point, able to sustain the outward force acting on the core [14]. In the following, this is achieved by suitably tailoring the input profiles $p_0(r)$ and $J_0^\phi(r)$.

Assuming up-down symmetry (reducing the algebra without changing the physics), the product of the Hessian eigenvalues along $\theta = \pi$ follows from Eq. (2) as

$$\lambda_r \lambda_\theta = \psi_0'' \hat{\psi}_{11} \varepsilon - (\hat{\psi}_{11} \hat{\psi}_{11}'' + 2\psi_0'' \hat{\psi}_{22}) \varepsilon^2 + \cdots \quad (7)$$

since $\hat{\psi}_{10}(r)$ and $\hat{\psi}_{21}(r)$ do vanish, the former due to $\hat{b}_{10}(r) = 0$ and the latter because all terms in $\hat{b}_{21}(r)$ are proportional to $\hat{\psi}_{10}(r)$ or to its derivatives [18]. Inserting $\hat{b}_{11}(r) = r^2[2r\dot{p}_0(r) - \psi_0'(r)]$ and $g_1(r) = \psi_0'(r)$ [10] into Eq. (5), one easily finds $\hat{\psi}_{11}(r_L)$ to be positive if $\dot{p}_0(r) > \frac{1}{2}\psi_0'(r)/r$ throughout $0 \le r \le r_L$, and negative otherwise, in case $\hat{b}_{11}(r)$ does not change its sign there. Since $\psi_0''(r_L) = J_0^\phi(r_L)$, on (r_L, π) and at first order in Eq. (7), a sufficiently hollow $p_0(r)$ leads to an x point ($\lambda_r \lambda_\theta < 0$), which may be turned into an o point ($\lambda_r \lambda_\theta > 0$) by flattening the pressure profile. Such flattening is, nevertheless, ineffective in removing the x point for elongated plasmas when oversimplified, null-gradient current-density models are considered. Indeed, setting $\dot{p}_0(r) = \dot{J}_0^\phi(r) = 0$, with negative current density $J^{(-)}$ flowing in the core and positive $J^{(+)}$ elsewhere [8], along with $r^{-1}\hat{b}_{22} = 2\hat{\psi}_{11} - (r^2\hat{\psi}_{11}')' - 2r^2\psi_0'$, yields at length

$$\hat{\psi}_{11}(r_L) = \frac{1}{16} r_L^3 J^{(+)}(\mu - 1 - 2\ln\mu), \quad (8a)$$

$$\hat{\psi}_{11}''(r_L) = \frac{1}{8} r_L J^{(+)}(\mu - 1), \quad (8b)$$

$$\hat{\psi}_{22}(r_L) = \frac{1}{32} r_L^2(\hat{\psi}_{22}^* + J^{(+)}), \quad (8c)$$

in the limit $r_L \ll 1$, where $\mu^{-1} = 1 - J^{(-)}/J^{(+)}$. The value $\hat{\psi}_{22}^*$ is related with the ellipticity κ^* at r_{22}^* through $\kappa^* \approx 1 + (\varepsilon/r_{22}^*)^2 \hat{\psi}_{22}^*/J^{(+)}$ [10], whence the condition

$$\kappa^* < 1 - \frac{1}{32}\left(\frac{\varepsilon}{r_{22}^*}\right)^2 \quad (9)$$

in order to keep $\lambda_r \lambda_\theta$ positive at (r_L, π).

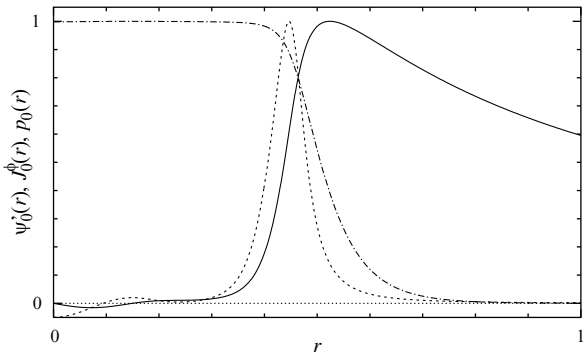

FIG. 1. Zeroth-order profiles $\psi_0'(r)$ (solid line), $J_0^\phi(r)$ (dashed line), and $p_0(r)$ for $\alpha = 9.5$ and $\gamma = 10$ (dashed-dotted line), normalized to their maximum values.

Enabling an o point at the low-field side for elongated plasmas requires more complex profiles. In terms of non-normalized poloidal flux $\Psi_0 = \psi_0 \Psi_{max}$, let

$$J_0^\phi(\Psi_0) \propto a_1 + a_2 \Psi_0 \quad (10a)$$

if $r \le r_L$, leading to $\psi_0 \propto 1 - J_0(j_{1,1} r/r_L)$, with $j_{1,1}$ the first zero of $J_1(x)$ and $J_\nu(x)$ Bessel functions of the first kind, and

$$J_0^\phi(\Psi_0) \propto \frac{b_1 + (\Psi_0 - \Psi_L)[b_2 - b_3 e^{-b_4(\Psi_0 - \Psi_L)}]}{1 + c_1(\Psi_0 - \Psi_L)^3 + c_2(\Psi_0 - \Psi_L)^4} \quad (10b)$$

elsewhere, taking $\Psi_L = \Psi_0(r_L)$. These are plotted in Fig. 1 for $a_1 = -0.2$ MA m^{-2}, $b_2 = 800$, $b_3 = b_4 = 1500$, $c_1 = 10^6$, and $c_2 = 3 \times 10^7$ [with $a_2 = -(j_{1,1}/r_L)^2$ and $b_1 = a_1 J_0(j_{1,1})$ chosen in order to ensure $\psi_0'(r_L) = 0$ and the continuity of $J_0^\phi(\psi_0)$ over $r_L = 0.15$], in addition to $\psi_0'(r)$, arising from Eq. (6) after rescaling $\Psi_0(r)$ by $\Psi_{max} = 0.46$ T m^2, and the normalized pressure model

$$p_0(\psi) = \varepsilon^2 A(1 + \alpha\psi) e^{-\gamma\psi} \quad (11)$$

with $A = 0.88$, all stemming from typical Joint European Torus parameters $a = 0.95$ m, $R_0 = 2.96$ m, $B_0 = 2.5$ T, $T_e = 6$ keV, $T_i = 1.8$ keV, $n_e = 1.5 \times 10^{19}$ m^{-3}, and $I_p \approx 1$ MA [3]. Contrary to previous works [8,9], the profiles in Eqs. (10) and (11) are not dictated by any limitation of the GS solver, their choice resulting only

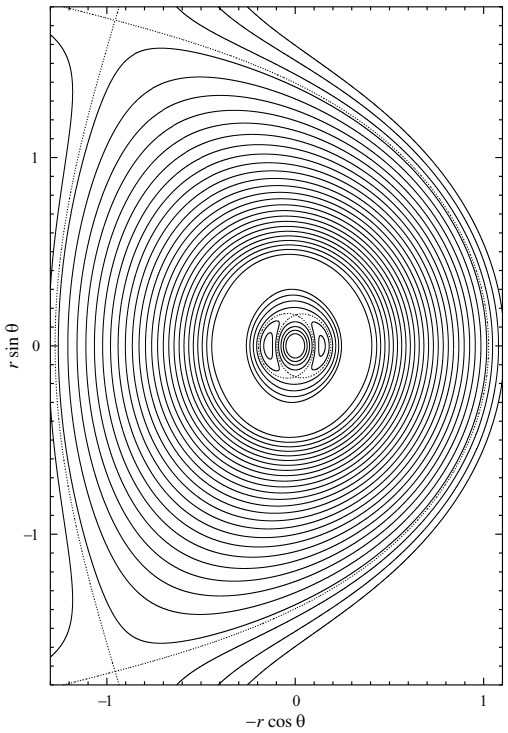

FIG. 2. Contours of $\psi(r, \theta) = -5(1 + i) \times 10^{-4}$ for $i = 1, \ldots, 6$ (core zone), $\psi(r, \theta) = i/20$ for $i = 1, \ldots, 28$ (outer zone), and the separatrices (dotted lines) for $\alpha = 9.5$ and $\gamma = 10$.

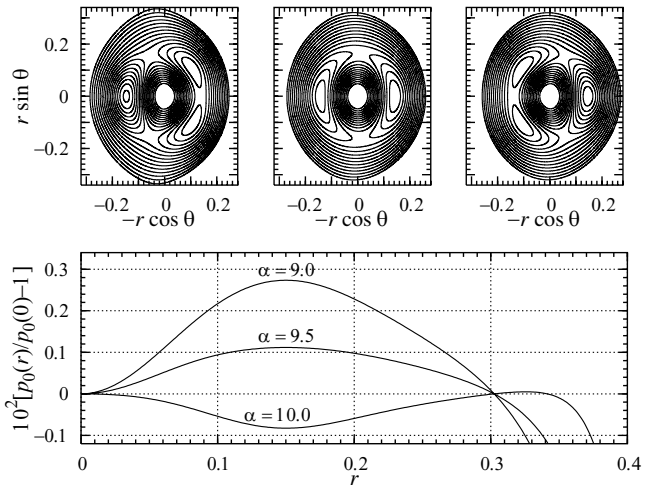

FIG. 3. Contours of $\psi(r,\theta) = -2(1+i)\times 10^{-4}$ for $i = 1,\ldots,19$ in the core for $\alpha = 9$, 9.5, and 10 (upper panel, from left to right) and corresponding profiles $10^2[p_0(r)/p_0(0) - 1]$ (lower panel, represented for $r \leq 0.4$ only).

from the wish to handle profiles as much reasonable and close to experiments as possible [3,4]. In fact, the model in Eq. (10b) is devised to provide a steep growth of $J_0^{\phi}(r)$ toward its main peak via the linear term in the numerator, followed by a drop to zero due to the denominator, while the exponential term accounts for a secondary peak at r_{L}. The equilibrium, for boundary conditions $\hat{\psi}_{22}(1) = 1.5$, $\hat{\psi}_{32}(1) = 4$, and $\hat{\psi}_{33}(1) = 5$, is depicted in Fig. 2, with two islands located over the midplane critical points. Pushed by surrounding positive-current channels, the negative-current core is limited to vertical motions only, which, in certain conditions, may be stabilized by the current flowing in the elongation coils [14]. Also, the effect of a variable pressure profile on the inner-separatrix shape is clearly illustrated in Fig. 3, where fine tuning α in Eq. (11) turns the low-field-side x point into an o point.

In conclusion, reversed equilibria were shown to be necessarily non-nested, except for the cylindrical case and other very particular degenerate configurations, and a perturbative approach was adapted to cope with a PFR layer and with generic profiles, disclosing some constraints they are subjected to. In particular, $\psi_0(r)$ was shown to be a solution of Eq. (6) rather than an arbitrary function with vanishing derivative at r_{L}, thus limiting the choices for the zeroth-order $B_0^{\theta}(r)$ [or, equivalently, $J_0^{\phi}(r)$], while the pressure, as any other continuously differentiable flux function, was found to be nonmonotonic over any chord of constant θ crossing the PFR layer. The ability to handle more general profiles enabled the x point at the low-field side to be changed into an o point for elongated plasmas, thus sustaining the negative-current core against outward forces from surrounding plasma currents and making its vertical displacements able to be stabilized by elongation-coil currents. Combined, these may prevent current redistribution aiming to restore a resilient-type current-density profile, which was shown to be incompatible with reversed configurations. Finally, in order to assess the physics of reversed equilibria, and even if experimental evidence of their existence remains an open issue, suitable GS solvers such as the one here presented (which is not bounded to any particular profile models and whose sole restrictions are the universal ones stemming from the GS equation) will always be required.

This work has been carried out within the framework of the Contract of Association between the European Atomic Energy Community and the Instituto Superior Técnico (IST), and has also received financial support from the Fundação para a Ciência e a Tecnologia (FCT). The content of this article is the sole responsibility of the authors and it does not necessarily represent the views of the European Commission, of FCT, of IST, or of their services.

*Electronic address: par@cfn.ist.utl.pt
†Electronic address: bizarro@cfn.ist.utl.pt

[1] N. C. Hawkes *et al.*, Phys. Rev. Lett. **87**, 115001 (2001).
[2] T. Fujita *et al.*, Phys. Rev. Lett. **87**, 245001 (2001).
[3] B. C. Stratton *et al.*, Plasma Phys. Controlled Fusion **44**, 1127 (2002).
[4] J. A. Breslau, S. C. Jardin, and W. Park, Phys. Plasmas **10**, 1665 (2003).
[5] J. M. Greene, J. L. Johnson, and K. E. Weimer, Phys. Fluids **14**, 671 (1971).
[6] M. S. Chu and P. B. Parks, Phys. Plasmas **9**, 5036 (2002).
[7] G. W. Hammett, S. C. Jardin, and B. C. Stratton, Phys. Plasmas **10**, 4048 (2003).
[8] A. A. Martynov, S. Y. Medvedev, and L. Villard, Phys. Rev. Lett. **91**, 085004 (2003).
[9] S. Wang, Phys. Rev. Lett. **93**, 155007 (2004).
[10] P. Rodrigues and J. P. S. Bizarro, Phys. Plasmas **11**, 186 (2004).
[11] D. Biskamp, Phys. Fluids **29**, 1520 (1986).
[12] J. B. Taylor, Phys. Fluids B **5**, 4378 (1993).
[13] D. Biskamp, Phys. Fluids B **5**, 3893 (1993).
[14] T. Takizuka, J. Plasma Fusion Res. **78**, 1282 (2002).
[15] R. Gilmore, *Catastrophe Theory for Scientists and Engineers* (John Wiley and Sons, New York, 1981), p. 51.
[16] D. P. L. Castrigiano and S. A. Hayes, *Catastrophe Theory* (Addison-Wesley, Reading, MA, 1993), p. 165.
[17] See, for instance, Fig. 5 in Ref. [4].
[18] Each term $\hat{b}_{nk}(r)$ is derived from the general expression Eq. (26) in Ref. [10] by setting $\mathcal{P}_n(r) = \mathcal{Y}_n(r) = 0$.